ACS OMEGA

http://pubs.acs.org/journal/acsodf

Article

Simultaneous Removal of Heavy Metals and Ciprofloxacin Micropollutants from Wastewater Using Ethylenediaminetetraacetic Acid-Functionalized β-Cyclodextrin-Chitosan Adsorbent

Monu Verma, Ingyu Lee, Shaveta Sharma, Ravi Kumar, Vinod Kumar, and Hyunook Kim*

Cite This: *ACS Omega* 2021, 6, 34624−34634

Read Online

ACCESS | Metrics & More | Article Recommendations | Supporting Information

ABSTRACT: The current study pertains to the synthesis of an EDTA-functionalized β-cyclodextrin-chitosan (β-CD-CS-EDTA) composite via a two-step process for the adsorptive removal of toxic heavy metallic ions (i.e., Pb(II), Cu(II), and Ni(II)) and antibiotic micropollutant, i.e., ciprofloxacin (CIP), from water. Different batch adsorption experiments such as pH, reaction time and initial pollutant concentration effects were carried out to identify the adsorption condition to attain the maximum removal efficiency. Kinetics results fit well with the pseudo-second order (PSO) kinetics model for both inorganic and organic pollutants. However, adsorption of heavy metal ions to the adsorbent was faster than that of CIP. Isotherms results showed excellent monolayer adsorption capacities of 330.90, 161, and 118.90 mg g^{-1} for Pb(II), Cu(II), and Ni(II), respectively, with a heterogeneous adsorption capacity of 25.40 mg g^{-1} for CIP. The adsorption mechanism was investigated using energy dispersive X-ray (EDX), elemental mapping, and Fourier transform infrared (FTIR) techniques. More significantly, the synthesized adsorbent gave good removal efficiencies when it was applied to simultaneously adsorb metal ions and CIP from real wastewater. Furthermore, excellent reusability could be obtained, making it a viable alternative to remove the inorganic and organic micropollutants for wastewater treatment.

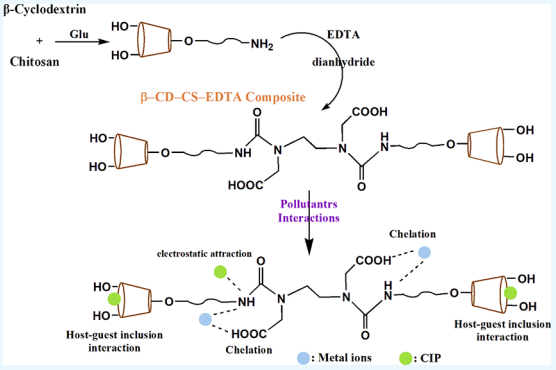

1. INTRODUCTION

Due to the rapid upsurge of industrial and agricultural activities along with rapid population growth, environmental pollution is becoming a serious threat for the quality of water and human health. Thousands of inorganic and organic micropollutants including heavy metal ions and pharmaceuticals are discharged into the water environment. The major dischargers of the pollutants include chemical manufacturing, metallurgical, mining, battery, and drug industries.[1−4] These pollutants are non-biodegradable, highly toxic, and carcinogenic for human and environmental health, especially when they are present in a complex mixture due to their different physiochemical properties.[5] Therefore, it is crucial to prepare a facile and environmentally friendly material that could efficiently remove both inorganic and organic micropollutants from wastewater.

Till now, various processes have been applied to effectively remove single or multi-components of organic or inorganic micropollutants from wastewater, for example, filtration, membrane separation, precipitation, adsorption, and reverse osmosis.[6−8] Among them, adsorption is considered as the most suitable method to remove coexisted micropollutants due to its ease in operation, lower cost, and higher adsorption capacity. Many literature studies have reported different types of adsorbents for the removal of a single class of inorganic and organic micropollutants from polluted water.[9,10] Previously, our research group also reported a few adsorption studies involving single class pollutants including metal ions and different dyes previously.[11−14] Apart from it, some efforts have been conducted to prepare a novel bifunctional or multifunctional adsorbent[15−18] to remove them simultaneously. Recently, Usman et al. synthesized a cross-linking polymer based on β-cyclodextrin(CD) and chitosan (CS) for the simultaneous removal of Hg(II), methylene blue (MB), and methyl orange (MO).[19] They reported the removal of MB by the host−guest-inclusion complex formation via β-CD cavities, while Hg(II) and MO were removed by the remaining functional groups such as hydroxyl, carboxyl, and amino groups of the adsorbent. Unfortunately, in practice, it is still difficult to simultaneously remove inorganic and organic pollutants from aqueous solution simply due to lower adsorption capacities and unavailability of selectivity of commercially available adsorb-

Received: September 10, 2021
Accepted: December 2, 2021
Published: December 13, 2021

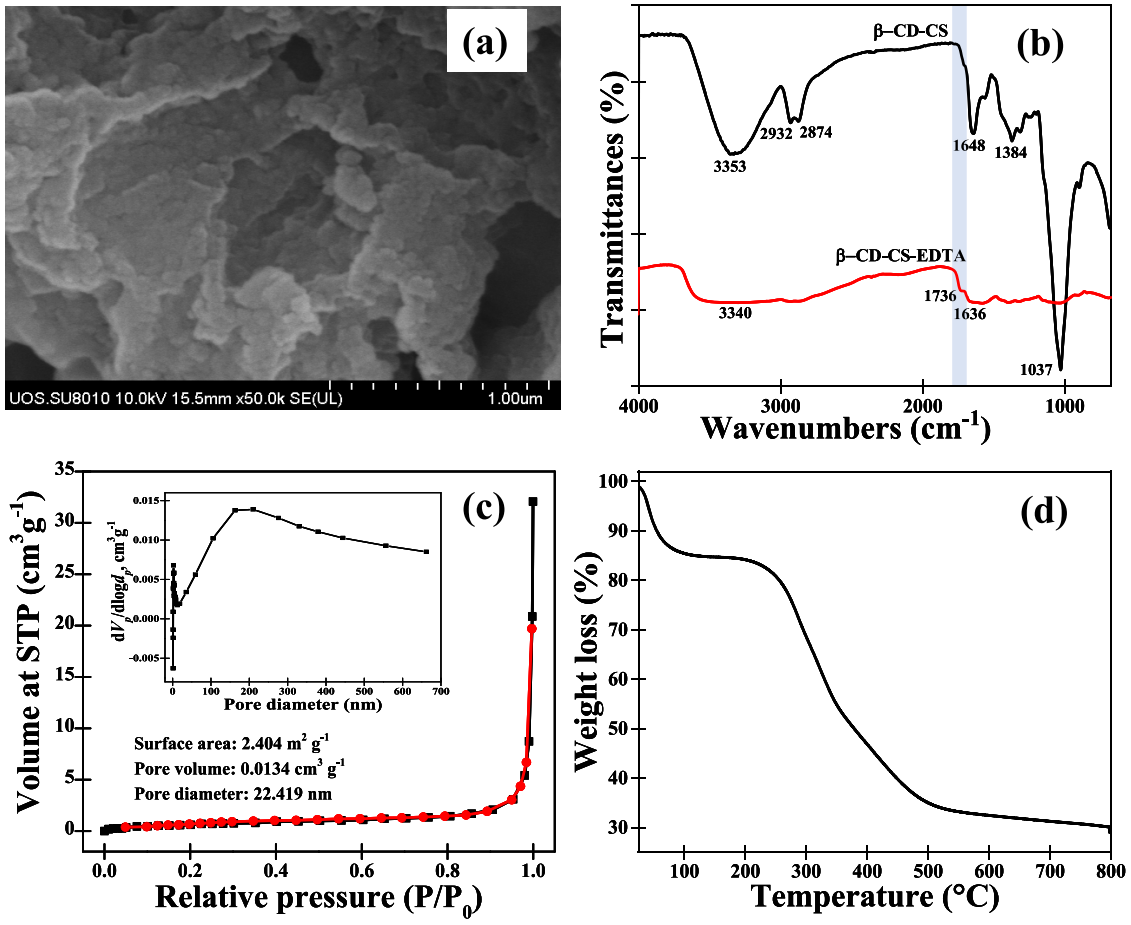

Figure 1. FESEM image (a), FTIR spectra (b), N_2 adsorption–desorption and inset pore size distribution (c), and TG data (d) for the β-CD-CS-EDTA adsorbent.

ents. To solve this issue, our research group[20] has also synthesized ethylenediaminetetraacetic acid (EDTA)-functionalized graphene-oxide (GO)-CS nanocomposites for the simultaneous adsorption of heavy metal ions and organic dyes and found that the material had an excellent adsorption capacity due to the existence of various active functional groups such as −COOH, −OH, $-NH_2$, etc. This study clearly demonstrated that multi-functional adsorption materials should be prepared for efficiently purifying wastewater that contains multiple types of pollutants.

Chitosan, a well-known deacetylated form of chitin is a natural linear chain polysaccharide material for adsorption. Chitosan possesses different properties such as good hydrophobicity, low toxicity, biodegradability, and miscibility with other polymers. In addition, it has a highly active structure with amino and hydroxyl groups, which makes it a potential candidate for polluted water treatment.[21,22] However, solubility in acid solution limits its use, so modification in its structure is necessary to extend its practical uses. β-CD, a seven-membered cyclic polysaccharide of glucose (α-D-glucopyranose) is produced via starch degradation by enzymes. It possesses a hydrophilic nature on its external surface and a hydrophobic nature in the internal cavity. The hydrophobic cavity makes it excellent in adsorbing different types of organic micropollutants through the so-called host–guest inclusion complex formation.[3,23] Also, the hydrophilic hydroxy groups have been modified by suitable functional groups to enhance its adsorption ability. Due to these properties, cross-linking of β-CD with chitosan was carried out to remove the inorganic and organic micropollutants simultaneously to take advantage of the superior adsorption properties coming from the components themselves and their synergism.[19,24,25] Recently, Li et al. reported the hyper-cross-linked β-CD porous polymer for the removal of aromatic micropollutants from water via the host–guest inclusion complexation of β-CD cavities.[26] However, due to inevitable competitions for free adsorption sites, these absorbents often encounter with inferior adsorption capacity and take a long time to attain adsorption equilibrium. Therefore, to enhance adsorption sites, doping the polymer with some suitable substances having more adsorption sites or specific functional groups is urgently needed.

Recently, the well-known chelating agent, EDTA is widely used in removing heavy metal ions through the hexadentate complex formation. Previously, different research groups have reported the functionalization of CS and β-CD with EDTA for the removal of single and multicomponent pollutants from wastewater.[17,27−30] More recently, our research group reported the trifunctional β–CD–EDTA–CS polymer using a simple and easy chemical route for the simultaneous removal of heavy metals, i.e., mercury (Hg^{2+}) and cadmium (Cd^{2+}), and organic dyes, i.e., methylene blue (MB), crystal violet (CV), and safranin O (SO), as inorganic and organic pollutants, respectively, and proposed the removal mechanism based on chelation, electrostatic interaction, and host–guest inclusion complex formation with β-CD cavities.[31] In this work, we also

https://doi.org/10.1021/acsomega.1c05015
ACS Omega 2021, 6, 34624−34634

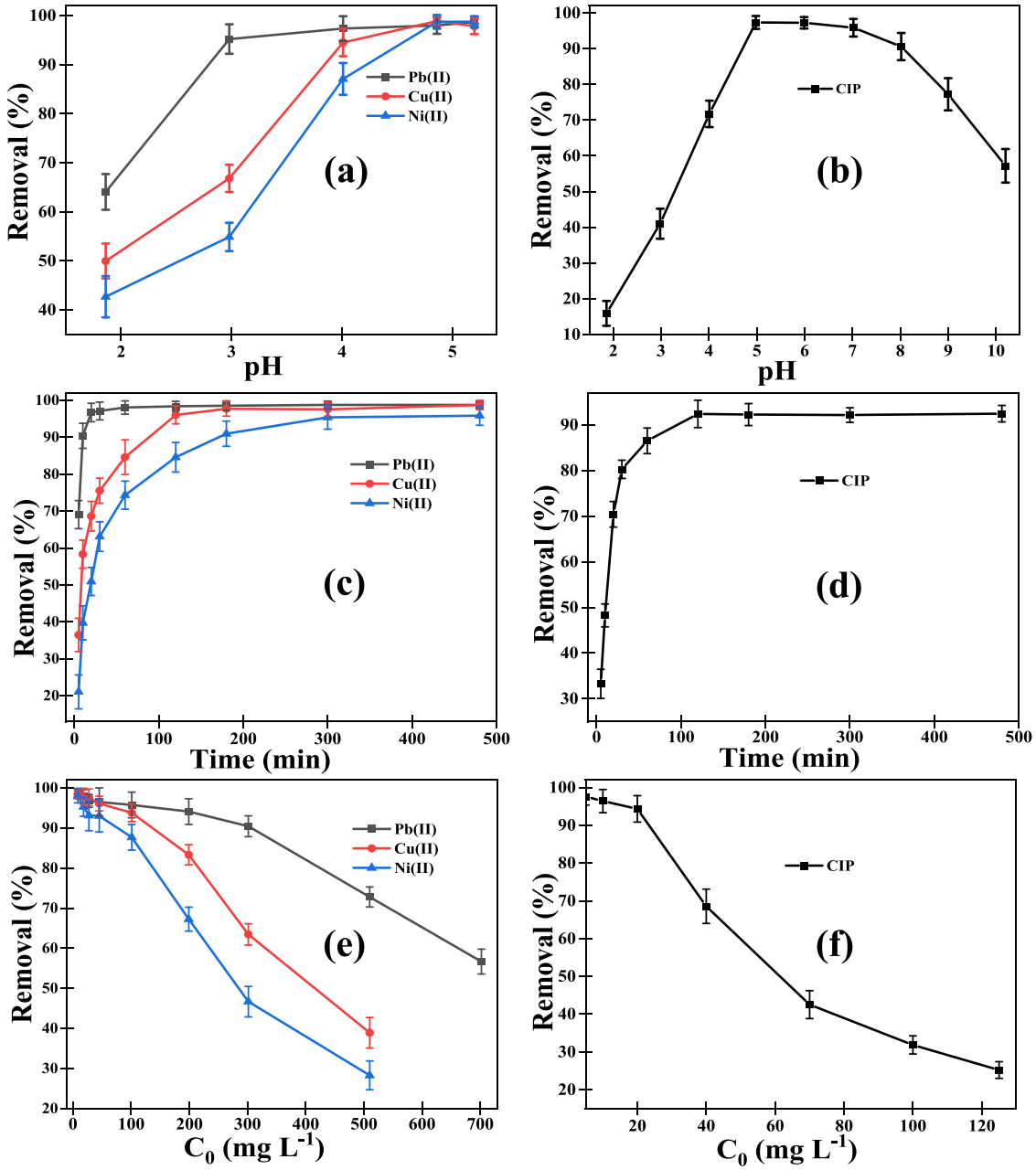

Figure 2. Effect of pH (a, b), contact time (c, d), and initial concentrations (e, f) on the removal efficiency of heavy metal ions and CIP, respectively, toward the β-CD-CS-EDTA composite.

reported the synergetic effect in the binary component system to show the enhancement in heavy metal adsorption.

In this work, an eco-friendly composite was prepared by modifying the β-CD-CS using EDTA via a two-step process and characterized using FT-IR, XRD, FESEM, EDX, BET, TGA, etc. The adsorption performance was investigated on most emerging pollutants: lead (Pb(II)), copper (Cu(II)), and nickel (Ni(II)) as model inorganic micropollutant and ciprofloxacin (CIP) as an organic micropollutant; they are often found in drinking water as well as industrial wastewater.[32] Different batch adsorption experiments such as pH, kinetics, isotherms, and reusability of the material for each micropollutant were examined on monocomponent systems. Lastly, the performance of the β−CD−CS−EDTA adsorbent was examined for the simultaneous removal of metal ions and CIP at environmental levels in real wastewater. The adsorption mechanism was investigated using elemental mapping, EDX, and FTIR spectra. To the best of our knowledge, no one has reported the use of β−CD−CS−EDTA synthesized via a two-step process for simultaneous removal of heavy metal ions and CIP micropollutants from wastewater. We believe that the current study delivers an alternate adsorbing material for the efficient removal of both classes of micropollutants from wastewater.

2. RESULTS AND DISCUSSION

2.1. Characterizations of β-CD-CS-EDTA. Figure 1a displays the surface morphology of the β-CD-CS-EDTA composite, which shows a highly smooth structure and confirms the successful introduction of EDTA dianhydride over the surface of β-CD-CS. The presence of different functional groups on β-CD-CS and β-CD-CS-EDTA was

https://doi.org/10.1021/acsomega.1c05015
ACS Omega 2021, 6, 34624−34634

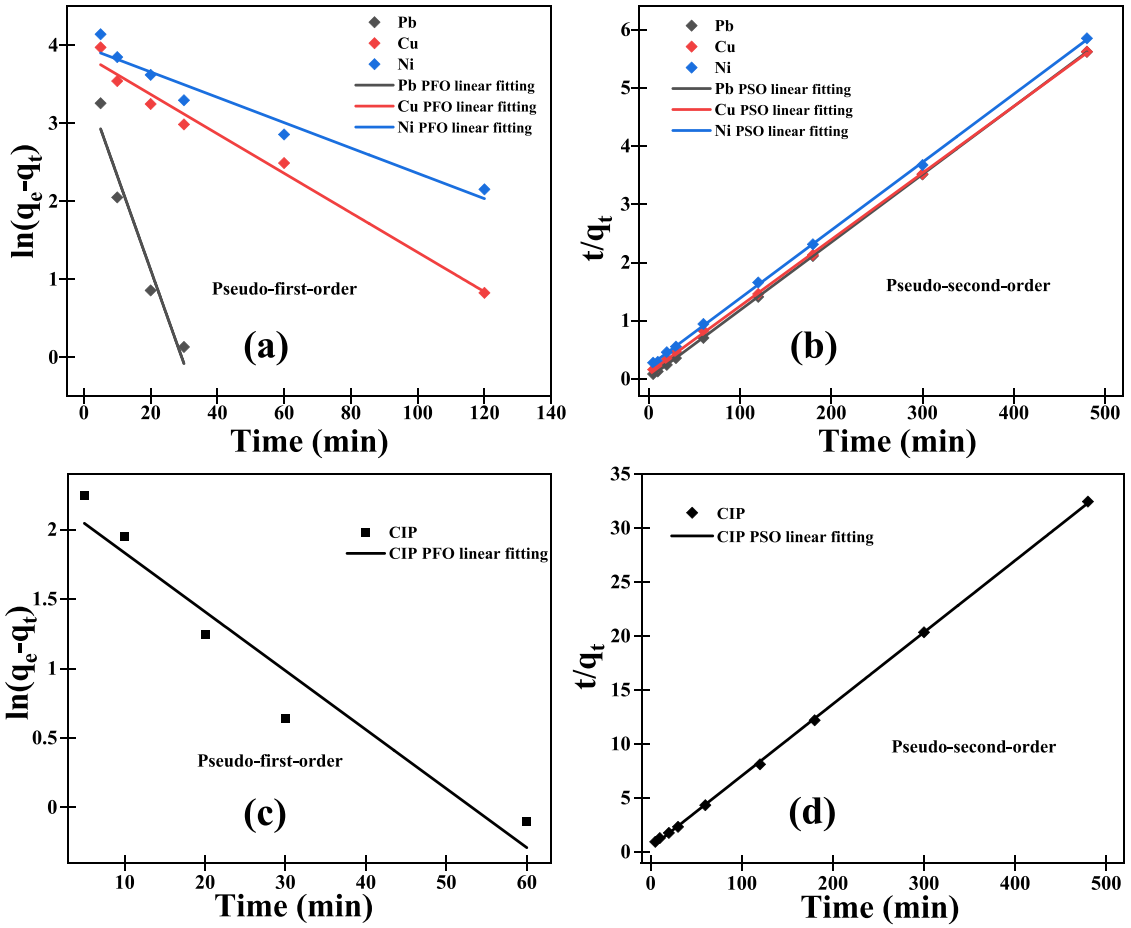

Figure 3. Linear kinetic modeling of PFO (a, c) and PSO (b, d) for heavy metal ions and CIP adsorption, respectively, on the β-CD-CS-EDTA composite.

confirmed by FTIR spectra, as shown in Figure 1b. In the spectrum of β-CD-CS, the broad adsorption peak situated at 3353 cm^{-1} occurred due to stretching vibrations of hydroxyl and amine (O−H and N−H) bands. The peaks situated at 2932 and 2874 cm^{-1} occurred due to the stretching vibration of C−H, 1648 cm^{-1} due to the bending vibration of N−H, and 1384 due to the bending vibration of the O−H group. Apart from them, one sharp peak situated at 1037 cm^{-1} could be observed, which was attributed to the antisymmetric vibration of the C−O−C bond.[33] This vibration peak suggests that the essential structure of β-CD was intact by the formation of the β-CD-CS product.[16] In the FTIR of the final product β-CD-CS-EDTA, two new peaks were observed at 1736 and 1635 cm^{-1}, which correspond to free carboxylic groups and the C═O stretching vibration of the amide I (−NHCO−) bond, respectively.[30] These two peaks confirm the successful grafting of EDTA on the β-CD-CS surface through the amide bond formation. The N_2 adsorption−desorption isotherm of the β-CD-CS-EDTA adsorbent at 77.4 K is presented in Figure 1c. Data indicating the H3 type hysteresis loop in the adsorption−desorption isotherm of the synthesized adsorbent suggest the capillary condensation presence and the existence of mesoporous materials. The surface area, pore volume, and pore diameter were calculated from the BET test and were found to be 2.404 $m^2\ g^{-1}$, 0.0134 $cm^3\ g^{-1}$, and 22.419 nm, respectively. Although the surface area and porosity values seem to be not sufficient for adsorption, still, adsorption efficiencies for the pollutants was not significantly affected since the adsorption mechanism is mainly related to the available functional groups on the adsorbent, not to the surface area.[34] The thermal stability of the β-CD-CS-EDTA was explored using TG analysis (Figure 1d), indicating three thermal-transition steps. These steps show the weight loss of 14.08, 24.73, and 30.87% in the range of 25−125, 160−330, and 330−800 °C, which correspond to the loss of water, decomposition of EDTA, and decomposition of polysaccharides (i.e., β-CD and chitosan), respectively.[16] XRD patterns of β-CD-CS and β-CD-CS-EDTA composites were shown in Figure S1. In β-CD-CS, only one broad peak was observed at 19.51° due to the presence of CS nature in the form of $-NH_2$ groups, which disappeared after the reaction with EDTA dianhydride and gave a broad peak only. This broad peak confirms the formation of the β-CD-CS-EDTA composite via the amide bond formation between the $-NH_2$ groups of β-CD-CS and EDTA dianhydride groups.

2.2. pH Effect. The existence of inorganic and organic micropollutants in an aqueous solution is also influenced by the acidity/basicity of the solution. Therefore, pH is an important factor in batch adsorption experiments for the removal of pollutants from polluted water. Figure 2a,b displays the removal efficiencies of metal ions and CIP at different pH values, respectively. The removal efficiencies of metal ions increased fast as pH increased and became unchanging above pH 4.86, and the maximum removal efficiencies were attained above pH 5. In the case of CIP, the removal efficiency was increased first up to 4.98, static in the range of pH 5.0−6.0 and

https://doi.org/10.1021/acsomega.1c05015
ACS Omega 2021, 6, 34624−34634

Table 1. Kinetics Model Parameters for the Adsorption of Heavy Metal Ions and CIP on the β-CD-CS-EDTA Adsorbent

		micropollutants			
models	parameters	Pb(II)	Cu(II)	Ni(II)	CIP
pseudo-first-order	$q_{m,exp}$ (mg g^{-1})	85.40	84.30	82.30	14.70
	$q_{e,cal}$ (mg g^{-1})	46.20	48.40	53.70	9.60
	k_1 (min^{-1})	0.120	0.025	0.015	0.004
	R^2	0.946	0.982	0.947	0.916
statistical tests	SSE	0.30	0.10	0.15	0.25
	SAE	1.0	0.70	0.80	0.80
	Δq	60.70	4.50	5.10	27.60
	χ^2	0.150	0.026	0.034	0.07
	mean error	0.40	0.20	0.20	030
pseudo-second-order	$q_{e,cal}$ (mg g^{-1})	86.20	87.70	85.50	15.20
	k_2 (g mg^{-1}·min^{-1})	12.30×10^{-3}	2.30×10^{-3}	1.60×10^{-3}	1.1×10^{-3}
	R^2	0.999	0.999	0.999	0.999
statistical tests	SSE	~0	~0	0.01	0.22
	SAE	0.10	0.2	0.20	1.20
	Δq	6.40	4.10	5.10	9.40
	χ^2	~0	~0	~0	0.03
	mean error	~0	~0	~0	0.20

then decreased continuously with increasing the value of solution pH. These behaviors can be explained with pH_{zpc}, which was calculated according to the previously reported pH drift method[35] and determined as 4.30 (Figure S2). Above this pH_{zpc}, the surface of the β-CD-CS-EDTA composite was negatively charged, while positively charged below this value, which means the adsorption would be highly affected by the system pH.

In the case of metal ion adsorption, when the solution pH was below 4.30, the surface of the β-CD-CS-EDTA composite was positively charged, which would create electrostatic repulsion with metal ions and give a less adsorption efficiency. With increasing pH, the surface became negatively charged and the electrostatic repulsion decreased, resulting in a higher adsorptive removal efficiency. Also, at a lower pH, the functional groups of the β-CD-CS-EDTA composite, i.e., −OH, −COOH, and $-NH_2$, were protonated and produced a positively charged surface due to which the competition between the H^+/H_3O^+ and positive-charged metal ions led to a lower adsorptive removal efficiency. As the pH increases, the positive charge of the surface became weaker, and the electrostatic interaction between the positively charged surface and metal ions increased, which gave a higher removal efficiency.[36,37]

The behavior of CIP adsorption was different from those of metal ions and can be explained on the two pKa values (pK_{a1} = 6.1 and pK_{a2} = 8.7) of CIP in water. CIP is positively charged below pH 6.1, while negatively charged above pH 8.7. Therefore, a lower adsorption efficiency could be observed at pH < pH_{zpc} simply because both CIP and the adsorbent surface were alike charged. However, a higher adsorption could be observed at pH between 4.30 and 6.0 since both CIP and the adsorbent surface were oppositely changed. Above pH 6.0, CIP was zwitterionic or anionic, resulting in the decreased interaction with the β-CD-CS-EDTA surface, which was negatively charged. Therefore, for both heavy metals and CIP adsorption, pH 5.20 was chosen for further experiments.

2.3. Effect of Contact Time and Kinetics. Figure 2 c,d shows the contact time effect on the removal efficiencies of heavy metals and CIP on β-CD-CS-EDTA, respectively. Data indicate the rapid adsorption in the initial 5−20 min for both pollutants, and then the uptake rates gradually decreased with the contact time increasing. The adsorption equilibrium could be attained within the initial 30−60 and 120 min for heavy metals and CIP, respectively. Therefore, 300 min was chosen as the excessive equilibrium time for the subsequent adsorption experiments.

To identify the adsorption rate and the rate-determining step, two famous kinetic models, which are pseudo-first order (PFO) and pseudo-second order (PSO), were applied for the kinetics data. Details of kinetic isotherms models are given in Text S1.

The linear fits for the PFO and PSO kinetics models are presented in Figure 3, and the calculated kinetics parameters along with different statistical values are listed in Table 1. For the PSO kinetics model, the fitting lines perfectly fit to the experimental data. Moreover, the parameters obtained from the model fits (Table 1) indicate that the PSO kinetics model would predict the data much better than the PFO kinetics model, as the $q_{e,cal}$ values obtained by the PSO were much closer to the experimental ones ($q_{m,exp}$) than those by the PFO kinetics model. Better coefficients of determinant (R^2 = 0.999) could be obtained by the PSO for both heavy metals and CIP. In fact, the χ^2 test also confirmed that the adsorption data would better follow the PSO kinetics than the PFO.

All these results suggest that the chemisorption was rate-determining in the adsorption process for both metal ions and CIP, and no mass transfer was involved in the adsorption mechanism.[30,38] This type of interaction describes the electronic sharing or transfer between the adsorbent and adsorbate and formation of chemical bonds in the adsorption process.[16] Table 1 also shows a faster adsorption kinetics (higher k_2 values) for metal ions than CIP, which indicates the higher availability of adsorption sites for inorganic pollutants (i.e., heavy metal ions) than organic pollutants (i.e., CIP) on β-CD-CS-EDTA. So, it can be easily presumed that EDTA plays a crucial and selective role in the adsorption of metallic ions. The faster adsorption in the beginning indicates that the chemical adsorption would be more important in both heavy metals and CIP adsorption.

2.4. Adsorption Isotherm. Figure 2e,f shows the effect of initial metal ions and CIP concentrations on the removal

https://doi.org/10.1021/acsomega.1c05015
ACS Omega 2021, 6, 34624−34634

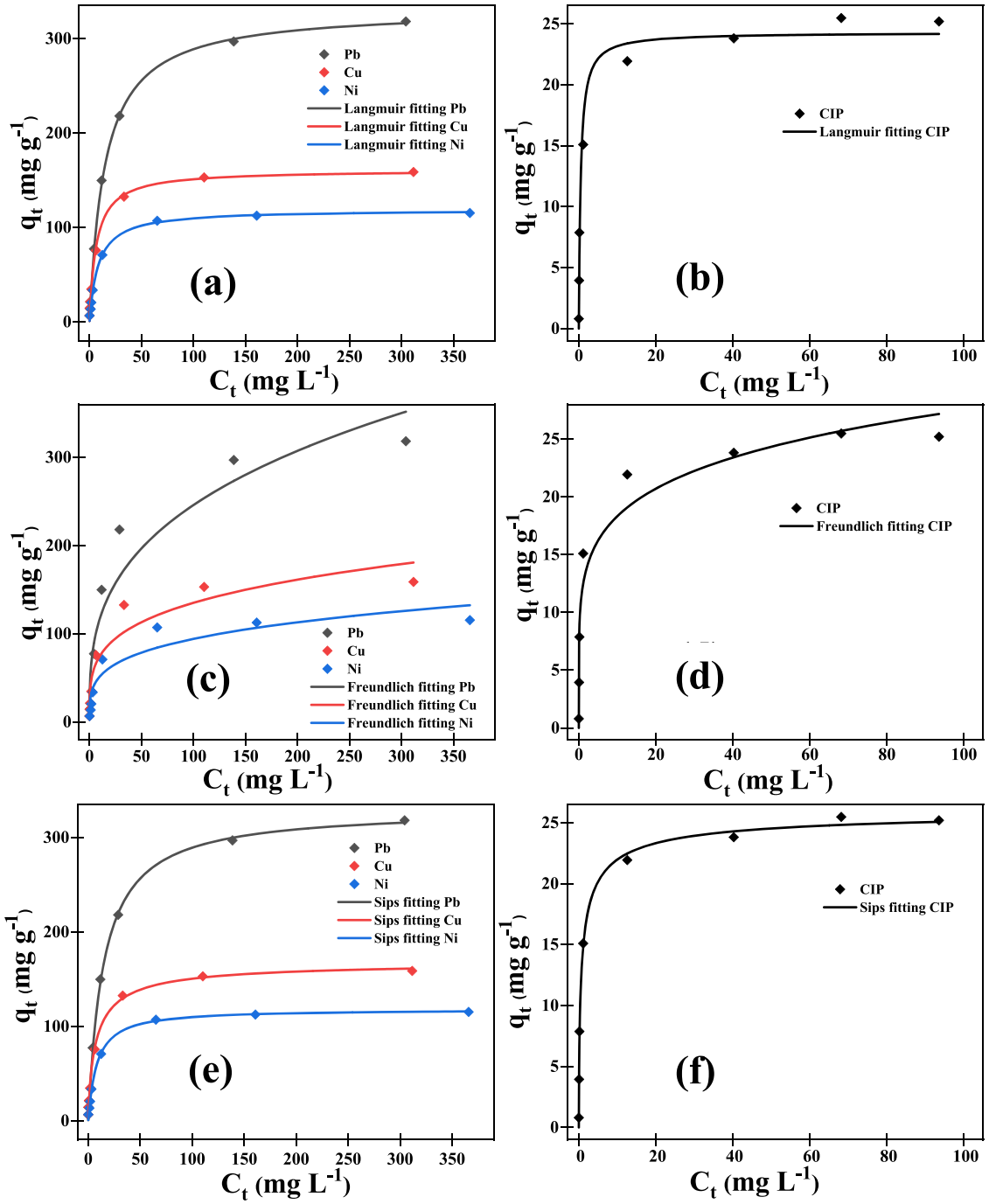

Figure 4. Non-linear isotherm Langmuir (a, b), Freundlich (c, d), and Sips (e, f) for heavy metal ions and CIP, respectively, on the *β*-CD-CS-EDTA composite.

efficiencies of the synthesized adsorbent. Figures indicate higher removal efficiencies at lower concentrations due to the availability of a larger number of active functional groups. The adsorption sites became eventually saturated as the initial concentration increases, which resulted in decreased removal efficiency.

To explain the relationship between the adsorbent and adsorbate at equilibrium, three different isotherms (i.e., Langmuir, Freundlich, and Sips models) were fit to the adsorption isotherm data. Details of the isotherm models are given in Text S2.

The non-linear fitting results for Langmuir, Freundlich, and Sips models corresponding to heavy metals and CIP micropollutants are shown in Figure 4, and different statistical parameters are listed in Table 2. From the isotherms tests, it was found that isotherms data better fit to the Langmuir or Sips model; the coefficients of determinant (R^2) for heavy metals and CIP were found to be >0.993 for both models. Also, the adsorption capacity ($q_{m,cal}$) values calculated by Langmuir and Sips models were found to be very close to the experimental adsorption capacity values ($q_{m,exp}$) of 320.20, 158.70, 115.40, and 25.20 mg L^{-1} for Pb(II), Cu(II), Ni(II), and CIP, respectively (Table 2). In short, better fitting results

https://doi.org/10.1021/acsomega.1c05015
ACS Omega 2021, 6, 34624−34634

Table 2. Adsorption Isotherm Parameters for Heavy Metal Ions and CIP on the β-CD-CS-EDTA Adsorbent

		water pollutants			
isotherm models	parameters	Pb(II)	Cu(II)	Ni(II)	CIP
Langmuir model	$q_{m,exp}$ (mg g^{-1})	320.20	158.70	115.40	25.20
	$q_{m,cal}$ (mg g^{-1})	330.90	161	118.90	24.30
	K_L (L mg^{-1})	0.066	0.153	0.119	2.060
	R^2	0.996	0.993	0.996	0.977
statistical tests	SSE	350.20	184.20	40.10	13.50
	SAE	43.70	29.50	12.80	9.50
	Δq	41.80	42.10	32.10	40.2
	mean error	7.10	5.50	2.60	1.50
Freundlich model	K_F (mg g^{-1})	55.898	41.485	28.279	12.215
	n	3.108	3.901	3.925	5.675
	R^2	0.930	0.915	0.895	0.943
statistical tests	SSE	8643.90	2477.0	1616.90	34.30
	SAE	254.60	131.0	103.40	13.50
	Δq	109.60	84.4	69.60	52.50
	mean error	35.1	20.3	16.40	2.40
Sips model	$q_{m,cal}$ (mg g^{-1})	330.10	169.10	118.20	25.40
	K_S (L mg^{-1})	0.068	0.129	0.122	1.337
	n_s	0.980	1.222	0.969	1.588
	R^2	0.994	0.992	0.996	0.995
statistical tests	SSE	346.70	94.50	38.70	2.90
	SAE	46.20	24.30	12.0	4.40
	Δq	42.40	29.30	32.60	38.90
	mean error	7	4.0	2.50	0.70

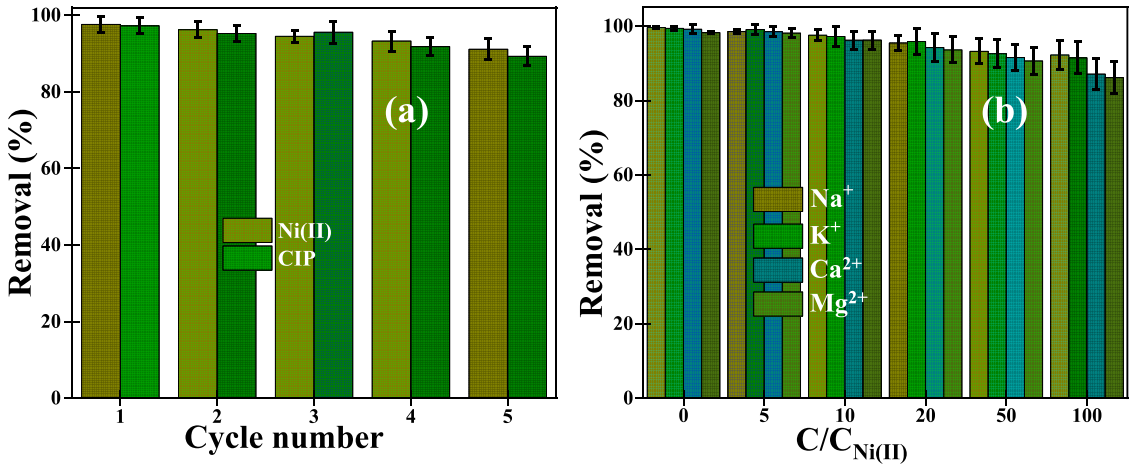

Figure 5. Regeneration efficiency of the β-CD-CS-EDTA composite for Ni(II) and CIP adsorption (a), and competing ion effect on the removal efficacy of Ni(II) (b) on the β-CD-CS-EDTA composite.

were obtained by the order of Langmuir > Sips > Freundlich for heavy metals and Sips > Langmuir > Freundlich for CIP. These results suggest the homogeneous distribution of adsorption active sites in the form of EDTA groups for heavy metals[39] while heterogeneous active sites in the form of β-CD cavities and EDTA for CIP on the surface of β-CD-CS-EDTA.[16] Additionally, the heterogeneity factor (n) for CIP was not equal to unity, which confirmed the heterogeneous adsorption. Table 2 also shows the higher K_L/K_S value for CIP than those for heavy metal ions, indicating the higher adsorption affinity of β-CD-CS-EDTA toward organic micropollutants in comparison to inorganic pollutants.[40]

2.5. Regeneration Study. The recycling and reusability of the used β-CD-CS-EDTA adsorbent are important parameters from the economic point of view. In this work, Ni(II)-loaded β-CD-CS-EDTA was regenerated using 1.0 M HNO_3, while CIP-loaded β-CD-CS-EDTA was regenerated using 5% HCl in ethanol according to a previous report.[17] Figure 5a shows the performance of the adsorbent during the five continuous adsorption−desorption cycles. Results indicate more than 97 and 95% removal efficiencies could be obtained initially for Ni(II)-loaded and CIP-loaded β-CD-CS-EDTA adsorbent, respectively. In fact, the adsorbent could maintain its adsorption capacity removal even after five cycles of adsorption desorption. Slightly declined removal efficiencies could be observed, 91 and 89% for Ni(II) and CIP, respectively. Therefore, the cost-effective synthesis, higher adsorption capacity, and good regeneration efficiency of the β-CD-CS-EDTA adsorbent makes it a potential candidate in practical wastewater treatment.

2.6. Effect of Interfering Ions. The effects of other ions' presence on the performance of the adsorbent were also tested.

https://doi.org/10.1021/acsomega.1c05015
ACS Omega 2021, 6, 34624−34634

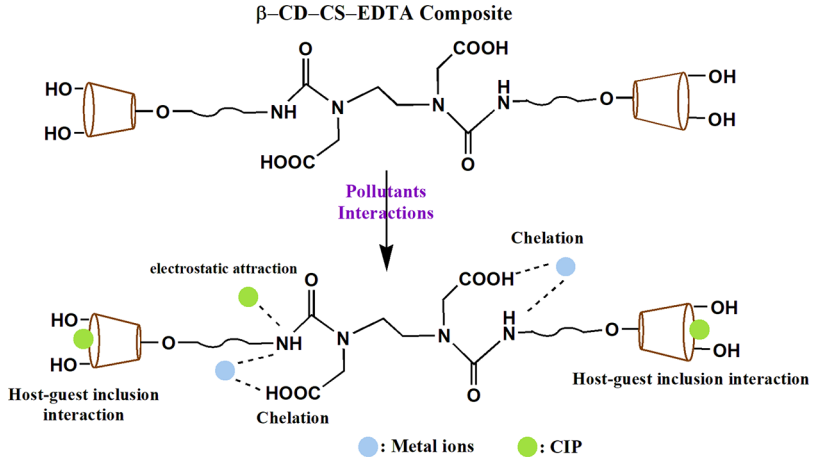

Figure 6. Mechanism for simultaneous adsorption of heavy metal ions and CIP.

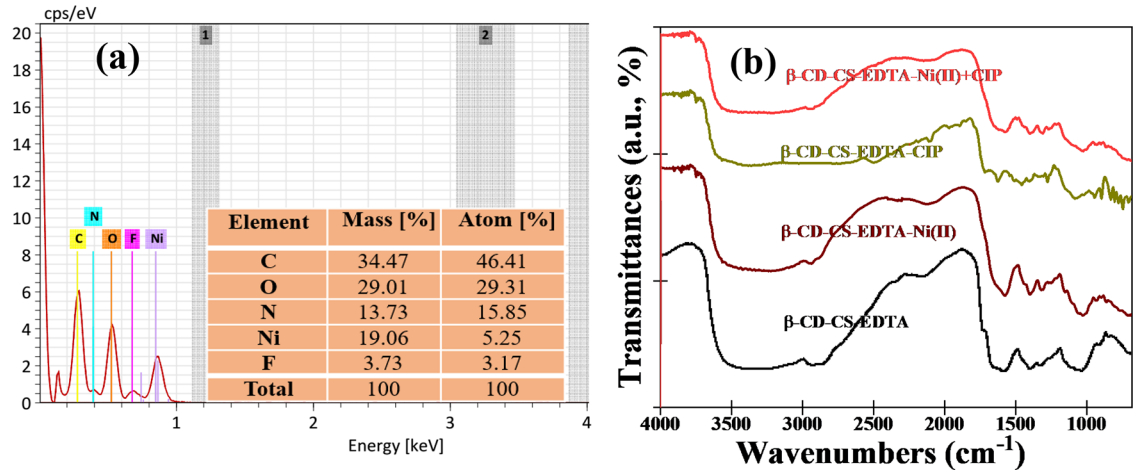

Figure 7. EDX and inset table indicates elemental composition after simultaneous adsorption of for Ni(II) and CIP (a). FTIR spectra of *β*-CD-CS-EDTA, Ni(II)-loaded *β*-CD-CS-EDTA, CIP-loaded *β*-CD-CS-EDTA, and simultaneous loaded Ni(II) and CIP (b).

For this specific study, Na^+, K^+, Ca^{2+}, and Mg^{2+} were selected as interfering ions due to their common existence in both natural water and wastewater from industrial sources. These interfering ions may negatively affect the adsorption performance of the adsorbent for target pollutants by competing with the available adsorption sites. Figure 5b displays the effects of the cations at different concentrations on the removal efficiency of the adsorbent for Ni(II). As shown in the figure, the removal efficiencies only slightly decreased for Ni(II) even at higher concentrations of the interfering ions. These results clearly indicate that the adsorptive performance of *β*-CD-CS-EDTA would hardly be affected by co-existing ions.

2.7. Adsorption Mechanism. Isotherm results clearly indicated that the excellent adsorption capacity of the *β*-CD-CS-EDTA adsorbent would mainly depend on the availability of a large number of available functional groups. Figure 6 demonstrates the possible adsorption mechanism for the adsorption of metal ions and CIP onto *β*-CD-CS-EDTA. According to the mechanism, the metal ions adsorbed to the adsorbent mainly via their chelation with EDTA and electrostatic interaction with −OH and $-NH_2$ groups of *β*-CD-CS-EDTA,[16] while CIP adsorbed via hydrogen bonding with −OH and $-NH_2$ groups (electrostatic attraction) and the inclusion-complex formation on *β*-CD cavities of the adsorbent, which is physical adsorption.[41]

The adsorption mechanism of the heavy metal ions and CIP pollutants were confirmed by EDX, elemental mapping, and FTIR spectra. Figure S3 shows the elemental mapping of the *β*-CD-CS-EDTA adsorbent after the simultaneous adsorption of Ni(II) and CIP. The colored elemental spots indicate the uniform distribution of Ni and CIP (F for ciprofloxacin) over the whole surface of the adsorbent, confirming the successful loading of metal ions and organic pollutants on the well-distributed adsorption sites on *β*-CD-CS-EDTA. The EDX spectrum along with elemental composition corresponding to elemental mapping is shown in Figure 7a, which clearly confirmed the higher adsorption of metal ions than CIP over the surface of the synthesized adsorbent, which strongly agrees with the isotherm adsorption data.

FTIR spectra of *β*-CD-CS-EDTA before and after the adsorption of pollutants Ni(II), CIP, and Ni(II) + CIP are compared in Figure 7b. In the Ni(II) adsorption case, the peak situated at 1736 cm^{-1} due to the −COOH group almost disappeared and the peaks situated at 3340 cm^{-1} due to O−H (or N−H) groups slightly shifted toward 3423 cm^{-1}, confirming the formation of chelation with EDTA and interaction with O−H (or N−H) groups with metal ions. In CIP adsorption, the O−H (or N−H) peak became broader, confirming the electrostatic interaction between F (i.e., CIP) and available functional groups. Apart from it, the character-

https://doi.org/10.1021/acsomega.1c05015
ACS Omega 2021, 6, 34624−34634

istic peak situated at 1037 cm^{-1} in β-CD-CS-EDTA, which was due to glucose,[15] shifted to 1023 cm^{-1} in β-CD-CS-EDTA-CIP confirming the host−guest inclusion complex formation with the β-CD as reported earlier for different organic pollutants.[3,42] The FTIR spectrum for Ni(II) + CIP adsorption shows the disappearance of carboxylic peaks and shifting in peaks of O−H/N−H and the glucose unit of the β-CD, confirming the adsorption of Ni(II) and CIP simultaneously through chelation, electrostatic interaction, and host−guest inclusion complex formation.

2.8. Performance of β-CD-CS-EDTA in Real Wastewater at Environmental Levels. The simultaneous removal of heavy metal ions and organic micropollutants was also investigated at an environmental level ($\mu g\ L^{-1}$) in real wastewater. The different physicochemical properties of collected wastewater are listed in Table S1.[20] The pH of the wastewater was adjusted to 5.10 by 0.1 M HNO_3, and then, different concentrations of Ni(II) and CIP were added to the wastewater to the levels that mostly cover all inorganic and organic pollutants concentrations in drinking water and wastewater. Figure 8 shows the good removal efficiency of

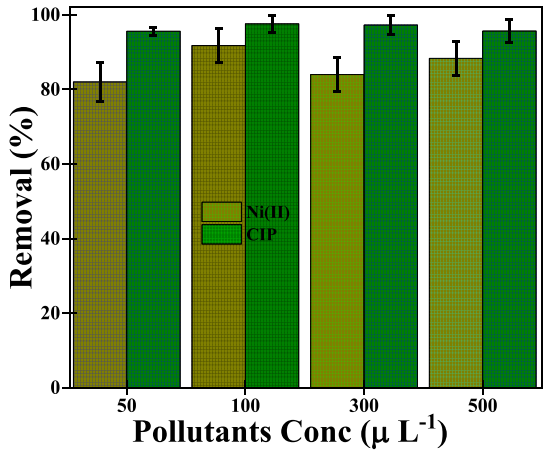

Figure 8. Adsorption performance of β-CD-CS-EDTA for the simultaneous removal of Ni(II) and CIP at environmentally level concentrations.

Ni(II) and CIP onto β-CD-CS-EDTA, demonstrating that the synthesized β-CD-CS-EDTA adsorbent could remove effectively both inorganic and organic micropollutants at the environmental level simultaneously.

Lastly, the adsorption performance of our synthesized β-CD-CS-EDTA composite was compared with those of previously reported adsorbents (Table S2). The table clearly shows that β-CD-CS-EDTA has the better adsorption capacity than the other reported adsorbents. Therefore, these results suggest that the β-CD-CS-EDTA adsorbent would be a promising adsorbent for the simultaneous removal of residual inorganic and organic micropollutants from wastewater.

3. CONCLUSIONS

In this study, we have synthesized a β-CD-CS-EDTA composite via a two-step simple and facile method and applied it for the adsorptive removal of Pb(II), Cu(II), Ni(II), and CIP from water. The different characteristics of the synthesized β-CD-CS-EDTA composite were described using FESEM, EDX, FTIR, XRD, TGA, and N_2 adsorption−desorption techniques. The maximum adsorption capacities of the β-CD-CS-EDTA composite for Pb(II), Cu(II), Ni(II), and CIP were determined to be 330.90, 161, 118.90, and 25.40 mg g^{-1}, respectively. The metal ions and CIP followed Langmuir and Sips isotherm models, confirming the homogeneous and heterogeneous adsorption characteristics, respectively. The adsorption of metal ions and CIP followed the PSO kinetics; adsorption of metal ions onto the adsorbent was faster than that of CIP. The faster adsorption and larger adsorption capacities of β-CD-CS-EDTA were due to the availability of a large number of active functional groups. The adsorption mechanism confirmed the heavy metal ion adsorption via chelation with EDTA of the adsorbent and electrostatic interaction with −OH and $-NH_2$ groups, while CIP adsorption occurred through electrostatic attraction and inclusion complex formation with β-CD cavities of the adsorbent. Moreover, the β-CD-CS-EDTA composite also produced a good simultaneous adsorption efficiency for the inorganic and organic pollutants, which co-existed in wastewater at the environmental level. Overall, the excellent adsorption capacity, synthetic simplicity, and better reusability of the adsorbent open the potential for the removal of both inorganic and organic micropollutants from wastewater.

4. MATERIALS AND METHODS

4.1. Materials. β-Cyclodextrin (β−CD, >97%), ethylenediaminetetraacetic acid (EDTA), and deacetylated chitosan flakes (+85%, the molecular weight and viscosity of the polymer were 190,000−375,000 g mol^{-1} and 200−2000 MPa, respectively) were supplied by Sigma-Aldrich (Seoul, South Korea). Glutaraldehyde (Glu, 50%) was purchased from Junsei (Kyoto, Japan). All other chemicals were of analytical grade and used without any further purification. pH was adjusted using 0.1 M HCl and 1 M NaOH.

4.2. Preparation of β-Cyclodextrin-Chitosan-EDTA (β-CD-CS-EDTA) Composite. The fabrication of the β-CD-CS-EDTA composite was carried out using a two-step process according to a previously reported modified method.[43] In the first step, the β-CD-CS composite was synthesized as follows: at first, 2.0 g CS and 12 g β-CD were dissolved in 250 mL of 1.0 M HCl solution, which was then stirred at 85−90 °C for 30 min. After that, 3.0 mL of glutaraldehyde was added to the solution with continuous stirring for 2.0 h. The solution pH was then adjusted to 8−9 with 1.0 M NaOH and continuously stirred for 30 min at the same temperature. Then, the solution was cooled and washed with ethanol and DI water and dried in a vacuum oven at 55 °C.

In the second step, dispersion of 2.0 g synthesized β-CD-CS was carried out in 50 mL of acetic acid (10%). Meanwhile, 15 g EDTA dianhydride synthesized by a previously reported method[44] was suspended in methanol. Then, both solutions were mixed at room temperature vigorously for 20 h. Thereafter, the solution was filtered and washed with 1.0 M NaOH to remove excess EDTA dianhydride. Finally, the harvested product was cleaned with ethanol and DI water and dried in a vacuum oven at 50 °C for harvesting. The harvested materials were ground properly for adsorption experiment.

4.3. Characterizations. All the characterization procedures are detailed in Text S3.

4.4. Batch Adsorption Experiments. All the batch adsorption experiments are detailed in Text S4.

4.5. Adsorption Performance of β-CD-CS-EDTA for Pollutants in Real Wastewater. Real wastewater samples were collected from the Jungnang Municipal Sewage Treat-

https://doi.org/10.1021/acsomega.1c05015
ACS Omega 2021, 6, 34624−34634

ment Plant, Seoul, South Korea. Their physicochemical analysis such as pH, alkalinity, dissolved oxygen (DO), total phosphorus (TP), total chemical oxygen demand (tCOD), soluble chemical oxygen demand (sCOD), total suspended solids (TSS), total Kjeldahl nitrogen (TKN), total ammonia nitrogen (TAN), etc., were determined following the standard methods (APHA, 2012).[20] In this wastewater, Ni(II) and CIP were added to adjust their concentrations to 50−500 μL^{-1}. Then, the adsorbent performance was evaluated with 50 mL of wastewater solution with a 50 mg adsorbent dose for 5 h of stirring time. The solution was separated, and existing concentrations of Ni(II) and CIP were analyzed by ICPE and LCMS spectrometers, respectively.

4.6. Statistical Tests. All the experiments were conducted three times under identical conditions. An Origin 2020 Pro (Microcal Software, Inc., USA) was used to calculate the margin error with a confidence interval of 95% for each set of the experiments. Different statistical parameters such as square sum of the errors (SSE), sum of absolute errors (SAE), reduced chi-square (χ^2), standard deviation Δq (%), and mean errors were also calculated.

■ ASSOCIATED CONTENT

Supporting Information

The Supporting Information is available free of charge at https://pubs.acs.org/doi/10.1021/acsomega.1c05015.

Kinetics models (Text S1), isotherm models (Text S2), characterizations (Text S3), batch adsorption experiments (Text S4), XRD patterns (Figure S1), pH_{pzc} (Figure S2), FESEM image and the EDX elemental distribution mapping of β-CD-CS-EDTA after simultaneous adsorption (Figure S3), physiochemical properties of used wastewater (Table S1), comparison of adsorption capacities with other reported adsorbents (Table S2), references (PDF)

■ AUTHOR INFORMATION

Corresponding Author

Hyunook Kim − *Water-Energy Nexus Laboratory, Department of Environmental Engineering, University of Seoul, Seoul 02504, Republic of Korea;* orcid.org/0000-0003-1256-480X; Email: h_kim@uos.ac.kr

Authors

Monu Verma − *Water-Energy Nexus Laboratory, Department of Environmental Engineering, University of Seoul, Seoul 02504, Republic of Korea;* orcid.org/0000-0001-8432-6160

Ingyu Lee − *Water-Energy Nexus Laboratory, Department of Environmental Engineering, University of Seoul, Seoul 02504, Republic of Korea*

Shaveta Sharma − *Water-Energy Nexus Laboratory, Department of Environmental Engineering, University of Seoul, Seoul 02504, Republic of Korea*

Ravi Kumar − *Department of Chemistry, National Institute of Technology Srinagar, Jammu & Kashmir 190006, India*

Vinod Kumar − *Department of Life Sciences, Graphic Era (Deemed to Be University), Dehradun, Uttarakhand 248002, India; Peoples' Friendship University of Russia (RUDN University), Moscow 117198, Russian Federation;* orcid.org/0000-0003-1808-1980

Complete contact information is available at: https://pubs.acs.org/10.1021/acsomega.1c05015

Notes

The authors declare no competing financial interest.

■ ACKNOWLEDGMENTS

M.V. thanks the National Research Foundation of Korea (NRF) for providing funding by the Ministry of Science and ICT by the BP Program (2019H1D3A1A01102657). H.K. was supported by Korea Environment Industry & Technology Institute through Post Plastic, a specialized program of the Graduate School funded by Korea Ministry of Environment (MOE). The RUDN University Strategic Academic Leadership Program also supported to this work.

■ REFERENCES

(1) Hong, Y.; Lee, I.; Lee, W.; Kim, H. Mass-Balance-Model-Based Evaluation of Sewage Treatment Plant Contribution to Residual Pharmaceuticals in Environmental Waters. *Chemosphere* **2019**, *225*, 378−387.

(2) An, T.; Yang, H.; Li, G.; Song, W.; Cooper, W. J.; Nie, X. Kinetics and Mechanism of Advanced Oxidation Processes (AOPs) in Degradation of Ciprofloxacin in Water. *Appl. Catal., B* **2010**, *94*, 288−294.

(3) Alsbaiee, A.; Smith, B. J.; Xiao, L.; Ling, Y.; Helbling, D. E.; Dichtel, W. R. Rapid Removal of Organic Micropollutants from Water by a Porous β-Cyclodextrin Polymer. *Nature* **2016**, *529*, 190−194.

(4) Sun, H.; Jiang, J.; Xiao, Y.; Du, J. Efficient Removal of Polycyclic Aromatic Hydrocarbons, Dyes, and Heavy Metal Ions by a Homopolymer Vesicle. *ACS Appl. Mater. Interfaces* **2018**, *10*, 713−722.

(5) Hu, X.; Xu, G.; Zhang, H.; Li, M.; Tu, Y.; Xie, X.; Zhu, Y.; Jiang, L.; Zhu, X.; Ji, X.; Li, Y.; Li, A. Multifunctional β-Cyclodextrin Polymer for Simultaneous Removal of Natural Organic Matter and Organic Micropollutants and Detrimental Microorganisms from Water. *ACS Appl. Mater. Interfaces* **2020**, *12*, 12165−12175.

(6) Qu, J.; Yuan, Y.; Meng, Q.; Zhang, G.; Deng, F.; Wang, L.; Tao, Y.; Jiang, Z.; Zhang, Y. Simultaneously Enhanced Removal and Stepwise Recovery of Atrazine and Pb(II) from Water Using β−Cyclodextrin Functionalized Cellulose: Characterization, Adsorptive Performance and Mechanism Exploration. *J. Hazard. Mater.* **2020**, *400*, 123142.

(7) Ajiboye, T. O.; Oyewo, O. A.; Onwudiwe, D. C. Simultaneous Removal of Organics and Heavy Metals from Industrial Wastewater: A Review. *Chemosphere* **2021**, *262*, 128379.

(8) Tran, H. N.; You, S. J.; Hosseini-Bandegharaei, A.; Chao, H. P. Mistakes and Inconsistencies Regarding Adsorption of Contaminants from Aqueous Solutions: A Critical Review. *Water Res.* **2017**, *120*, 88−116.

(9) Sun, Y.; Xu, L.; Jin, P.; Bai, X.; Jin, X.; Shi, X. Simultaneous Removal of Colorless Micropollutants and Hexavalent Chromium by Pristine TiO_2 under Visible Light: An Electron Transfer Mechanism. *Chem. Eng. J.* **2021**, *405*, 126968.

(10) Yap, P. L.; Nine, M. J.; Hassan, K.; Tung, T. T.; Tran, D. N. H.; Losic, D. Graphene-Based Sorbents for Multipollutants Removal in Water: A Review of Recent Progress. *Adv. Funct. Mater.* **2021**, *31*, 2007356.

(11) Verma, M.; Kumar, A.; Singh, K. P.; Kumar, R.; Kumar, V.; Srivastava, C. M.; Rawat, V.; Rao, G.; Kumari, S.; Sharma, P.; Kim, H. Graphene Oxide-Manganese Ferrite (GO-$MnFe_2O_4$) Nanocomposite: One-Pot Hydrothermal Synthesis and Its Use for Adsorptive Removal of Pb_{2+} Ions from Aqueous Medium. *J. Mol. Liq.* **2020**, *315*, 113769.

(12) Verma, M.; Mitan, M.; Kim, H.; Vaya, D. Efficient Photocatalytic Degradation of Malachite Green Dye Using Facilely Synthesized Cobalt Oxide Nanomaterials Using Citric Acid and Oleic Acid. *J. Phys. Chem. Solids* **2021**, *155*, 110125.

(13) Verma, M.; Tyagi, I.; Kumar, V.; Goel, S.; Vaya, D.; Kim, H. Fabrication of GO−MnO_2 Nanocomposite Using Hydrothermal Process for Cationic and Anionic Dyes Adsorption: Kinetics, Isotherm, and Reusability. *J. Environ. Chem. Eng.* **2021**, *9*, 106045.
(14) Jaiswal, K. K.; Kumar, V.; Vlaskin, M. S.; Nanda, M.; Verma, M.; Ahmad, W.; Kim, H. Hydropyrolysis of Freshwater Macroalgal Bloom for Bio-Oil and Biochar Production: Kinetics and Isotherm for Removal of Multiple Heavy Metals. *Environ. Technol. Innovation* **2021**, *22*, 101440.
(15) Qin, X.; Bai, L.; Tan, Y.; Li, L.; Song, F.; Wang, Y. β-Cyclodextrin-Crosslinked Polymeric Adsorbent for Simultaneous Removal and Stepwise Recovery of Organic Dyes and Heavy Metal Ions: Fabrication, Performance and Mechanisms. *Chem. Eng. J.* **2019**, *372*, 1007−1018.
(16) Zhao, F.; Repo, E.; Yin, D.; Chen, L.; Kalliola, S.; Tang, J.; Iakovleva, E.; Tam, K. C.; Sillanpää, M. One-Pot Synthesis of Trifunctional Chitosan-EDTA-β-Cyclodextrin Polymer for Simultaneous Removal of Metals and Organic Micropollutants /. *Sci. Rep.* **2017**, *7*, 15811.
(17) Zhao, F.; Repo, E.; Yin, D.; Meng, Y.; Jafari, S.; Sillanpa, M. EDTA-Cross-Linked B-Cyclodextrin: An Environmentally Friendly Bifunctional Adsorbent for Simultaneous Adsorption of Metals and Cationic Dyes. *Environ. Sci. Technol.* **2015**, *49*, 10570−10580.
(18) Chen, M.; Bi, R.; Zhang, R.; Yang, F.; Chen, F. Tunable Surface Charge and Hydrophilicity of Sodium Polyacrylate Intercalated Layered Double Hydroxide for Efficient Removal of Dyes and Heavy Metal Ions. *Colloids Surf., A* **2021**, *617*, 126384.
(19) Usman, M.; Ahmed, A.; Yu, B.; Wang, S.; Shen, Y.; Cong, H. Simultaneous Adsorption of Heavy Metals and Organic Dyes by β-Cyclodextrin-Chitosan Based Cross-Linked Adsorbent. *Carbohydr. Polym.* **2021**, *255*, 117486.
(20) Verma, M.; Lee, I.; Oh, J.; Kumar, V.; Kim, H. Synthesis of EDTA-Functionalized Graphene Oxide-Chitosan Nanocomposite for Simultaneous Removal of Inorganic and Organic Pollutants from Complex Wastewater. *Chemosphere* **2022**, *287*, 132385.
(21) Zheng, X.; Zheng, H.; Xiong, Z.; Zhao, R.; Liu, Y.; Zhao, C.; Zheng, C. Novel Anionic Polyacrylamide-Modify-Chitosan Magnetic Composite Nanoparticles with Excellent Adsorption Capacity for Cationic Dyes and PH-Independent Adsorption Capability for Metal Ions. *Chem. Eng. J.* **2020**, *392*, 123706.
(22) Biswas, S.; Fatema, J.; Debnath, T.; Rashid, T. U. Chitosan−Clay Composites for Wastewater Treatment: A State-of-the-Art Review. *ACS EST Water* **2021**, 1055−1085.
(23) Schofield, W. C. E.; Bain, C. D.; Badyal, J. P. S. Cyclodextrin-Functionalized Hierarchical Porous Architectures for High-Throughput Capture and Release of Organic Pollutants from Wastewater. *Chem. Mater.* **2012**, *24*, 1645−1653.
(24) Kekes, T.; Tzia, C. Adsorption of Indigo Carmine on Functional Chitosan and β-Cyclodextrin/Chitosan Beads: Equilibrium, Kinetics and Mechanism Studies. *J. Environ. Manage.* **2020**, *262*, 110372.
(25) Karpkird, T.; Manaprasertsak, A.; Penkitti, A.; Sinthuvanich, C.; Singchuwong, T.; Leepasert, T. A Novel Chitosan-Citric Acid Crosslinked Beta-Cyclodextrin Nanocarriers for Insoluble Drug Delivery. *Carbohydr. Res.* **2020**, *498*, 108184.
(26) Li, H.; Meng, B.; Chai, S. H.; Liu, H.; Dai, S. Hyper-Crosslinked β-Cyclodextrin Porous Polymer: An Adsorption-Facilitated Molecular Catalyst Support for Transformation of Water-Soluble Aromatic Molecules. *Chem. Sci.* **2016**, *7*, 905−909.
(27) Zhao, F.; Repo, E.; Sillanpää, M.; Meng, Y.; Yin, D.; Tang, W. Z. Green Synthesis of Magnetic EDTA- And/or DTPA-Cross-Linked Chitosan Adsorbents for Highly Efficient Removal of Metals. *Ind. Eng. Chem. Res.* **2015**, *54*, 1271−1281.
(28) Roosen, J.; Binnemans, K. Adsorption and Chromatographic Separation of Rare Earths with EDTA- and DTPA-Functionalized Chitosan Biopolymers. *J. Mater. Chem. A* **2014**, *2*, 1530−1540.
(29) Zhao, F.; Repo, E.; Meng, Y.; Wang, X.; Yin, D.; Sillanpää, M. An EDTA-β-Cyclodextrin Material for the Adsorption of Rare Earth Elements and Its Application in Preconcentration of Rare Earth Elements in Seawater. *J. Colloid Interface Sci.* **2016**, *465*, 215−224.
(30) Wu, D.; Hu, L.; Wang, Y.; Wei, Q.; Yan, L.; Yan, T.; Li, Y.; Du, B. EDTA Modified β-Cyclodextrin/Chitosan for Rapid Removal of Pb(II) and Acid Red from Aqueous Solution. *J. Colloid Interface Sci.* **2018**, *523*, 56−64.
(31) Verma, M.; Lee, I.; Hong, Y.; Kumar, V.; Kim, H. Multifunctional β-Cyclodextrin-EDTA-Chitosan Polymer Adsorbent Synthesis for Simultaneous Removal of Heavy Metals and Organic Dyes from Wastewater. *Environ. Pollut.* **2022**, *292*, 118447.
(32) Pei, Z.; Shan, X. Q.; Kong, J.; Wen, B.; Owens, G. Coadsorption of Ciprofloxacin and Cu(II) on Montmorillonite and Kaolinite as Affected by Solution PH. *Environ. Sci. Technol.* **2010**, *44*, 915−920.
(33) Fan, L.; Luo, C.; Sun, M.; Qiu, H.; Li, X. Synthesis of Magnetic β-Cyclodextrin-Chitosan/Graphene Oxide as Nanoadsorbent and Its Application in Dye Adsorption and Removal. *Colloids Surf., B* **2013**, *103*, 601−607.
(34) Kayaci, F.; Aytac, Z.; Uyar, T. Surface Modification of Electrospun Polyester Nanofibers with Cyclodextrin Polymer for the Removal of Phenanthrene from Aqueous Solution. *J. Hazard. Mater.* **2013**, *261*, 286−294.
(35) Verma, M.; Tyagi, I.; Chandra, R.; Gupta, V. K. Adsorptive Removal of Pb (II) Ions from Aqueous Solution Using CuO Nanoparticles Synthesized by Sputtering Method. *J. Mol. Liq.* **2017**, *225*, 936−944.
(36) Kumar, K.; Kumar, V.; Verma, R.; Verma, M.; Kumar, A.; Vlaskin, M. S.; Nanda, M.; Kim, H. Graphitic Bio-Char and Bio-Oil Synthesis via Hydrothermal Carbonization-Co-Liquefaction of Microalgae Biomass (Oiled/de-Oiled) and Multiple Heavy Metals Remediations. *J. Hazard. Mater.* **2021**, *409*, 124987.
(37) Cui, L.; Wang, Y.; Gao, L.; Hu, L.; Yan, L.; Wei, Q.; Du, B. EDTA Functionalized Magnetic Graphene Oxide for Removal of Pb(II), Hg(II) and Cu(II) in Water Treatment: Adsorption Mechanism and Separation Property. *Chem. Eng. J.* **2015**, *281*, 1−10.
(38) Guo, X.; Du, B.; Wei, Q.; Yang, J.; Hu, L.; Yan, L.; Xu, W. Synthesis of Amino Functionalized Magnetic Graphenes Composite Material and Its Application to Remove Cr (VI), Pb (II), Hg (II), Cd (II) and Ni (II) from Contaminated Water. *J. Hazard. Mater.* **2014**, *278*, 211−220.
(39) Li, B.; Zhang, Y.; Ma, D.; Shi, Z.; Ma, S. Mercury Nano-Trap for Effective and Efficient Removal of Mercury(II) from Aqueous Solution. *Nat. Commun.* **2014**, *5*, 5537.
(40) Liu, H.; Cai, X.; Wang, Y.; Chen, J. Adsorption Mechanism-Based Screening of Cyclodextrin Polymers for Adsorption and Separation of Pesticides from Water. *Water Res.* **2011**, *45*, 3499−3511.
(41) Hussein, K.; Türk, M.; Wahl, M. A. Comparative Evaluation of Ibuprofen/β-Cyclodextrin Complexes Obtained by Supercritical Carbon Dioxide and Other Conventional Methods. *Pharm. Res.* **2007**, *24*, 585−592.
(42) Zhou, Y.; Hu, Y.; Huang, W.; Cheng, G.; Cui, C.; Lu, J. A Novel Amphoteric β-Cyclodextrin-Based Adsorbent for Simultaneous Removal of Cationic/Anionic Dyes and Bisphenol A. *Chem. Eng. J.* **2018**, *341*, 47−57.
(43) Wang, Y.; Wu, X.; Zhang, W.; Huang, S. One-Pot Synthesis of $MnFe_2O_4$ Nanoparticles-Decorated Reduced Graphene Oxide for Enhanced Microwave Absorption Properties. *Mater. Technol.* **2017**, *32*, 32−37.
(44) Tülü, M.; Geckeler, K. E. Synthesis and Properties of Hydrophilic Polymers. Part 7. Preparation, Characterization and Metal Complexation of Carboxy-Functional Polyesters Based on Poly(Ethylene Glycol). *Polym. Int.* **1999**, *48*, 909−914.

https://doi.org/10.1021/acsomega.1c05015
ACS Omega 2021, 6, 34624−34634